Determination of P-wave anisotropic parameters and thickness of a single layer of arbitrary anisotropy from traveltimes of a reflected P wave

Han Xiao [1] and Ivan Pšenčík [2,3]

[1]College of Geo-Exploration Science and Technology, Jilin University, Changchun, China, E-mail: 1184918974@qq.com
[2]Institute of Geophysics, Acad. Sci. of CR, Boční II, 141 31 Praha 4, Czech Republic. E-mail: ip@ig.cas.cz
[3]Charles University, Faculty of Mathematics and Physics, Department of Geophysics, Ke Karlovu 3, 121 16 Praha 2, Czech Republic

Summary

We present an inversion scheme allowing estimates of the thickness of a layer and its parameters from traveltimes of the wave reflected from the bottom of the layer. We concentrate on unconverted P wave reflected in a homogeneous layer of arbitrary anisotropy symmetry and orientation. The inversion scheme is based on the approximate traveltime formula derived under the assumption of weak anisotropy. For the description of anisotropy, the so-called A-parameters, which represent an alternative to standard elastic moduli specifying anisotropic media, are used. Nine of fifteen P-wave A-parameters, which describe P-wave propagation in weak-anisotropy approximation, can be determined. The thickness of the layer may be either a sought or known quantity. If an additional information about the orientation of symmetry elements is available for higher-symmetry anisotropy, the corresponding phase-velocity surface can be reconstructed. Synthetic tests indicate that the inversion scheme works very well for weak anisotropy (less than 10%), yields reasonable results even for anisotropy stronger than 20%. The scheme has tendency to overestimate the thickness of the layer if it is a sought parameter.

Introduction

There are various approaches to the parameter estimation from reflection moveout data in media of varying anisotropy. For their overall description, see Tsvankin and Grechka (2011). Our approach differs from these approaches in several respects. First of all, we concentrate on only traveltimes of reflected unconverted P waves. In this respect, our parameter estimation differs from, for example, parameter estimation of Grechka et al. (2005) who also use traveltimes of reflected S waves. Second, we concentrate on weakly-to-moderately anisotropic media. In this respect, our approach is similar to that used by Xiao et al. (2004), who tested various P-wave moveout approximations, but only in VTI layers, and used them for the estimate of Thomsen (1986) parameters. Our approach is applicable to anisotropy of any symmetry and orientation. The use of weak-anisotropy approximation allows us to use simple linear relations between traveltimes and anisotropy

Seismic Waves in Complex 3–D Structures, **30** (2020), 9–28 (ISSN 2336–3827, online at http://sw3d.cz)

parameters (Pšenčík and Farra, 2017). We make no a priori assumptions about anisotropy symmetry, we always seek all parameters, which can be obtained from the inversion of traveltimes of reflected waves. Third, in addition to anisotropy parameters we may also seek the thickness of the layer, in which reflection occurs.

For the parameterization of an anisotropic medium, we use the so-called A-parameters, see Pšenčík et al., (2018, 2020). Because we concentrate on P waves only, we are unable to estimate all 21 anisotropy parameters characterizing the medium. Without additional information, we are often even unable to estimate all fifteen P-wave anisotropy parameters, which describe P-wave propagation in the weak-anisotropy approximation.

In the study, we consider the Cartesian coordinate system z_i, whose z_3 axis is vertical, positive downwards. The axes z_1 and z_2 are situated in the horizontal plane so that the coordinate system is right-handed. We call the system *global* in order to distinguish it from other used coordinate systems as, for example, *profile* or *crystal* coordinate systems. The profile coordinate system shares its vertical axis with the global coordinate system, its horizontal axes may be rotated with respect to the axes of the global coordinate system. The coordinate planes or axes of the crystal coordinate system coincide with the symmetry elements of the studied anisotropy medium.

The structure of the paper is following. We present an approximate formula for the calculation of traveltimes of a P wave reflected at the bottom of a homogeneous layer of arbitrary anisotropy. Traveltimes are recorded on a horizontal surface representing the top of the layer. The formula is modified into two alternative forms, which can be used in the inversion scheme. After a brief description of the inversion scheme, results of several synthetic inversion tests on models of varying anisotropy symmetry and strength are presented. The paper ends by a short conclusion section. In Appendices, a reader may find definitions of involved A-parameters and their transformation rules (Appendix A), brief description of the inversion scheme (Appendix B) and specification of anisotropy parameters used in synthetic tests (Appendix C).

Theoretical background

Traveltime formula

We start from equation (16) of Pšenčík and Farra (2017), which provides an approximate expression for the traveltime T of the P wave reflected from the bottom of a single homogeneous layer of arbitrary anisotropy and orientation, recorded along a horizontal profile. The mentioned equation was derived under the weak-anisotropy approximation. Within it, the following assumptions were made. The actual ray of the reflected wave was replaced by a nearby reference ray in a reference isotropic medium. The deviation of the reference ray from the actual ray was considered to be of the first order. The traveltime along it then represents the first-order approximation of the actual traveltime (Fermat principle). Instead of exact ray and phase velocities, their first-order weak-anisotropy approximations (Farra and Pšenčík, 2016) were used. In this approximation, ray and phase velocities are assumed to be equal. Another approximation is the omission of six anisotropy parameters whose effect on traveltimes of reflected P wave are negligible, see more details below. In equation (16) of Pšenčík and Farra (2017), the so-called weak-anisotropy (WA) parameters were used. Here we replace them by A-parameters, see Pšenčík et al. (2018, 2020).

Equation (16) of Pšenčík and Farra (2017) for the traveltime T along a horizontal profile reads:

$$T^2(x) = T_0^2 \frac{(1+\bar{x}^2)^3}{P(\bar{x})} \ . \tag{1}$$

The symbol $\bar{x}$ denotes the normalized offset and T_0 the two-way zero-offset traveltime. They are given by equations:

$$\bar{x} = \frac{x}{2H} \ , \qquad T_0 = \frac{2H}{\alpha} \ . \tag{2}$$

Here H is the thickness of the layer and α is the reference P-wave velocity of the reference isotropic medium. It should be chosen so that it makes the A-parameters small. The symbol $P(x)$ in equation (1) is the polynomial:

$$P(x) = (1+x^2)^2 + 2\epsilon_x^P x^4 + 2(\epsilon_x^P + \eta_y^P + \epsilon_z^P)x^2 + 2\epsilon_z^P. \tag{3}$$

The parameters ϵ_x^P, η_y^P and ϵ_z^P represent *profile* A-parameters defined in Appendix A. They describe anisotropy in the vertical plane containing the profile. We use indices P to distinguish the profile A-parameters from *global* A-parameters (without indices) defined also in Appendix A. Let us assume that the considered profile makes an angle φ with z_1 axis of the global coordinate system. Then the profile A-parameters ϵ_x^P, η_y^P and ϵ_z^P can be expressed in terms of nine global A-parameters in the way shown in equation (A-4). The values of all A-parameters depend on the choice of the P-wave reference velocity α; equation (1) is, however, *independent* of α.

After inserting equation (A-3) expressing the profile A-parameters in terms of global A-parameters to equation (3), the polynomial $P(x)$ attains the following form:

$$\begin{aligned} P(x) = (1+x^2)^2 + 2(&\epsilon_x \cos^2\varphi + \epsilon_y \sin^2\varphi + \eta_z \cos^2\varphi \sin^2\varphi \\ &+2\chi_z \cos\varphi \sin\varphi - 2\epsilon_{16} \cos^3\varphi \sin\varphi - 2\epsilon_{26} \cos\varphi \sin^3\varphi)x^4 \\ &+2(\eta_x \sin^2\varphi + \eta_y \cos^2\varphi + \epsilon_x \cos^2\varphi + \epsilon_y \sin^2\varphi + \epsilon_z + 2\chi_z \cos\varphi \sin\varphi)x^2 + 2\epsilon_z \ . \end{aligned} \tag{4}$$

Equation (4) thus depends on nine of fifteen P-wave global A-parameters, which describe P-wave propagation in weakly anisotropic approximation. The dependence of equation (4) on remaining six P-wave A-parameters is negligible, see Pšenčík and Farra (2017).

For the purpose of the inversion, i.e., for the determination of global A-parameters from the observed traveltimes T_{obs} of P-wave reflected from the bottom of the layer, it is useful to rewrite equation (1) to the following form:

$$\begin{aligned} &\epsilon_x \bar{x}^2(1+\bar{x}^2)\cos^2\varphi + \epsilon_y \bar{x}^2(1+\bar{x}^2)\sin^2\varphi + \epsilon_z(1+\bar{x}^2) + 2\chi_z \bar{x}^2(1+\bar{x}^2)\cos\varphi\sin\varphi \\ &+\eta_x \bar{x}^2 \sin^2\varphi + \eta_y \bar{x}^2 \cos^2\varphi + \eta_z \bar{x}^4 \cos^2\varphi \sin^2\varphi \\ &-2\xi_{16}\bar{x}^4 \cos^3\varphi \sin\varphi - 2\xi_{26}\bar{x}^4 \cos\varphi \sin^3\varphi = \tfrac{1}{2}(1+\bar{x}^2)^2\left[\tfrac{T_0^2(1+\bar{x}^2)}{T_{obs}^2(x)} - 1\right] \ . \end{aligned} \tag{5}$$

As equation (1), equation (5) is also independent of the reference velocity α. We can, therefore, choose any reasonable value of α and consider it known. In this way, equation (5) contains ten unknowns: nine A-parameters and the thickness H of the layer. The number of unknown A-parameters can be reduced by one if we realize that for the offset $x = 0$, equation (5) yields:

$$\epsilon_z = \frac{1}{2}\frac{T_0^2 - T_{obs}^2(0)}{T_{obs}^2(0)} \ . \tag{6}$$

Thus ϵ_z can be determined independently of the remaining eight A-parameters. In such a case, equation (5) reduces to:

$$\begin{aligned}
&\epsilon_x \bar{x}^2(1+\bar{x}^2)\cos^2\varphi + \epsilon_y \bar{x}^2(1+\bar{x}^2)\sin^2\varphi + 2\chi_z \bar{x}^2(1+\bar{x}^2)\cos\varphi\sin\varphi \\
&+\eta_x \bar{x}^2\sin^2\varphi + \eta_y \bar{x}^2\cos^2\varphi + \eta_z \bar{x}^4\cos^2\varphi\sin^2\varphi \\
&-2\xi_{16}\bar{x}^4\cos^3\varphi\sin\varphi - 2\xi_{26}\bar{x}^4\cos\varphi\sin^3\varphi \\
&= \tfrac{1}{2}(1+\bar{x}^2)\Big[\Big(\tfrac{T_0^2(1+\bar{x}^2)}{T_{obs}^2(x)} - 1\Big)(1+\bar{x}^2) - \Big(\tfrac{T_0^2 - T_{obs}^2(0)}{T_{obs}^2(0)}\Big)\Big] \ .
\end{aligned} \tag{7}$$

In the inversion, we can thus use equation (5) for nine unknown A-parameters or equation (7) for eight unknown A-parameters, and ϵ_z can be determined form equation (6). In the following, we use the latter option.

Inversion scheme

Equation 7 for N source-receiver pairs can be arranged in the form of a system of N linear equations to determine eight unknown P-wave A-parameters from N observed reflected P-wave traveltimes T_{obs} corresponding to N offsets x. In the matrix form we can write:

$$\mathbf{G}\mathbf{m} = \mathbf{d} \ . \tag{8}$$

Here, $\mathbf{G}$ represents an $N \times M$ matrix, where N is the number of receivers and M is the number of sought A-parameters, in our case $M = 8$. The rows of matrix $\mathbf{G}$ have the form shown in equation (B-2). Each row in matrix $\mathbf{G}$ corresponds to one particular offset. Symbol $\mathbf{m}$ in equation (8) denotes the vector of model parameters to be determined. In our case, it consists of eight P-wave A-parameters, see equation (B-3) (ϵ_z is determined independently from equation (6)). Vector $\mathbf{d}$ in equation (8) contains known quantities, as observed traveltimes T_{obs}, normalized offsets $\bar{x}$ and the zero-offset traveltime T_0. The explicit form of the vector $\mathbf{d}$ is given in equation (B-4).

Equation (8) is solved by means of pseudoinverse described in Appendix B, see equations (B-5) to (B-8).

In order to estimate the thickness H of the studied layer, we successively invert equation (8) for varying values of H in the interval of their expected values. For each value of H, we estimate eight A-parameters ϵ_x, ϵ_y, η_x, η_y, η_z, ξ_{16}, ξ_{26} and χ_z by solving equation (8) and ϵ_z from equation (6). We insert estimated values into equation (1), and seek the

value of H, which minimizes the average relative traveltime error

$$T_{AV} = N^{-1} \sum_{i=1}^{N} |T(x_i) - T_{obs}(x_i)|/T_{obs}(x_i) \times 100\% \ . \tag{9}$$

Here N is again the number of used receivers.

Synthetic tests

The above-described procedure is applied to P-wave traveltimes calculated by program package ANRAY (Gajewski and Pšenčík, 1990) and considered as observed traveltimes T_{obs}. They are generated by the source situated at the center of an 8×8 km region, and recorded by 51 receivers irregularly distributed in the region, see Figure 1. One of the receivers is situated in the center of the 8×8 km region and allows measurement of the zero-offset traveltime. The reference velocity α of the reference isotropic medium is chosen as $\alpha = 3.6$ km/s in all tests. Anisotropy of varying type of symmetry, strength and orientation is considered. The anisotropy strength is defined as $2(c_{max} - c_{min})/(c_{max} + c_{min})\times 100\%$, where c_{max} and c_{min} denote maximum and minimum phase velocities. Traveltimes generated by the package ANRAY with no added noise, and with added random Gaussian noise of 2 ms and 4 ms are inverted.

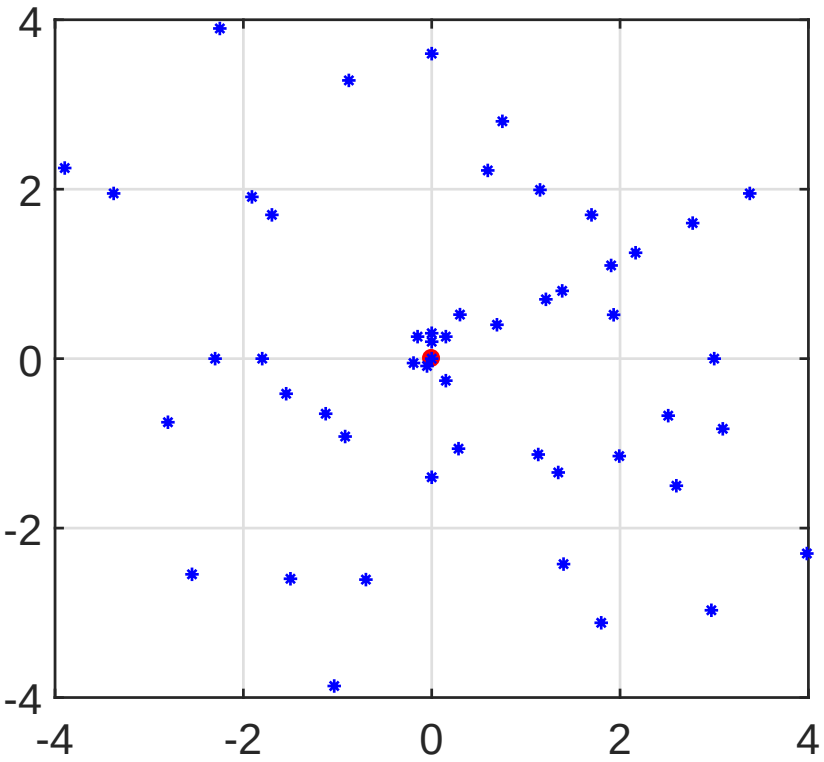

Figure 1: Distribution of 50 irregularly distributed surface sources around the wellhead (red full circle; $x = y = 0$ km), at which reflection traveltimes used for the inversion are recorded.

First we test the described procedure on reflection traveltimes obtained in a homogeneous isotropic layer. The use of noiseless and 2 ms data leads to a perfect estimate of

the thickness of the layer and of A-parameters. A-parameters ϵ_x, ϵ_y and ϵ_z are equal, A-parameters η_x, η_y and η_z are zero, which clearly indicates isotropy of the layer. Inversion of data with 4 ms noise leads to a slight overestimate of the thickness H of the layer, and small errors in estimated A-parameters. But it is still clear that the considered layer is isotropic.

In the next test, Model A, we invert traveltimes of the wave reflected from the bottom of a weakly transversely isotropic layer with the vertical axis of symmetry (VTI layer). The thickness of the layer is $H = 0.6$ km. The material considered is limestone (Pšenčík and Farra, 2017), its anisotropy is about 8%. The 6×6 matrix of the density normalized elastic moduli in the crystal coordinate system in Voigt notation is shown in equation (C-1). Corresponding nine involved A-parameters are shown in Table 1 as true parameters.

Model A	ϵ_x	ϵ_y	ϵ_z	η_x	η_y
	η_z	χ_z	ξ_{16}	ξ_{26}	
True	-0.100	-0.100	-0.153	0.040	0.040
$H = 0.6$ km	0.	0.	0.	0.	
Estimated	-0.101	-0.098	-0.260	-0.049	-0.029
$H = 0.5$ km	-0.002	-0.005	-0.004	-0.005	
Estimated	-0.101	-0.098	-0.154	0.032	0.039
$H = 0.6$ km	-0.002	-0.003	-0.003	-0.004	
Estimated	-0.102	-0.099	-0.029	0.030	0.042
$H = 0.7$ km	-0.002	-0.001	0.	-0.002	
Estimated	-0.102	-0.099	0.115	-0.045	-0.034
$H = 0.8$ km	-0.002	0.	0.	-0.001	

Table 1: True parameters and parameters estimated by inversion of traveltimes with 2 ms random Gaussian noise added to the data generated by ANRAY package in the model A. A-parameters ϵ_x, ϵ_y, ϵ_z, η_x, η_y, η_z, χ_z, ϵ_{16} and ϵ_{26} estimated for varying thickness of the layer H. P-wave reference velocity $\alpha = 3.6$ km/s.

In Figure 2, we illustrate the procedure of the search for the thickness H of the studied layer. Figure 2 shows the plots of relative traveltime differences $(T_H - T_{obs})/T_{obs}$ as a function of the offset with a) noiseless data, b) data with 2 ms random noise, and c) data with 4 ms random noise. Traveltime T_H is calculated from equation (1), in which inverted A-parameters and the assumed thickness H of the layer are used. Four thickness values are tested in Figure 2, H=0.5, 0.6, 0.7 and 0.8 km. Each value of H is related to a different symbol. Red symbols are used for such H, for which $T = T_H$ in equation (9) yields minimum T_{AV}. In Figures 2a and 2b, minimum T_{AV} is obtained for H=0.6 km, which is the true thickness. As in isotropic layers, increasing noise increases chances for overestimate of H. This is possible to see in Figure 2c, in which the noise level of 4 ms leads to the overestimation of the thickness of the layer H to $H = 0.7$ or $H = 0.8$ km (both values of H yield the same value of T_{AV}).

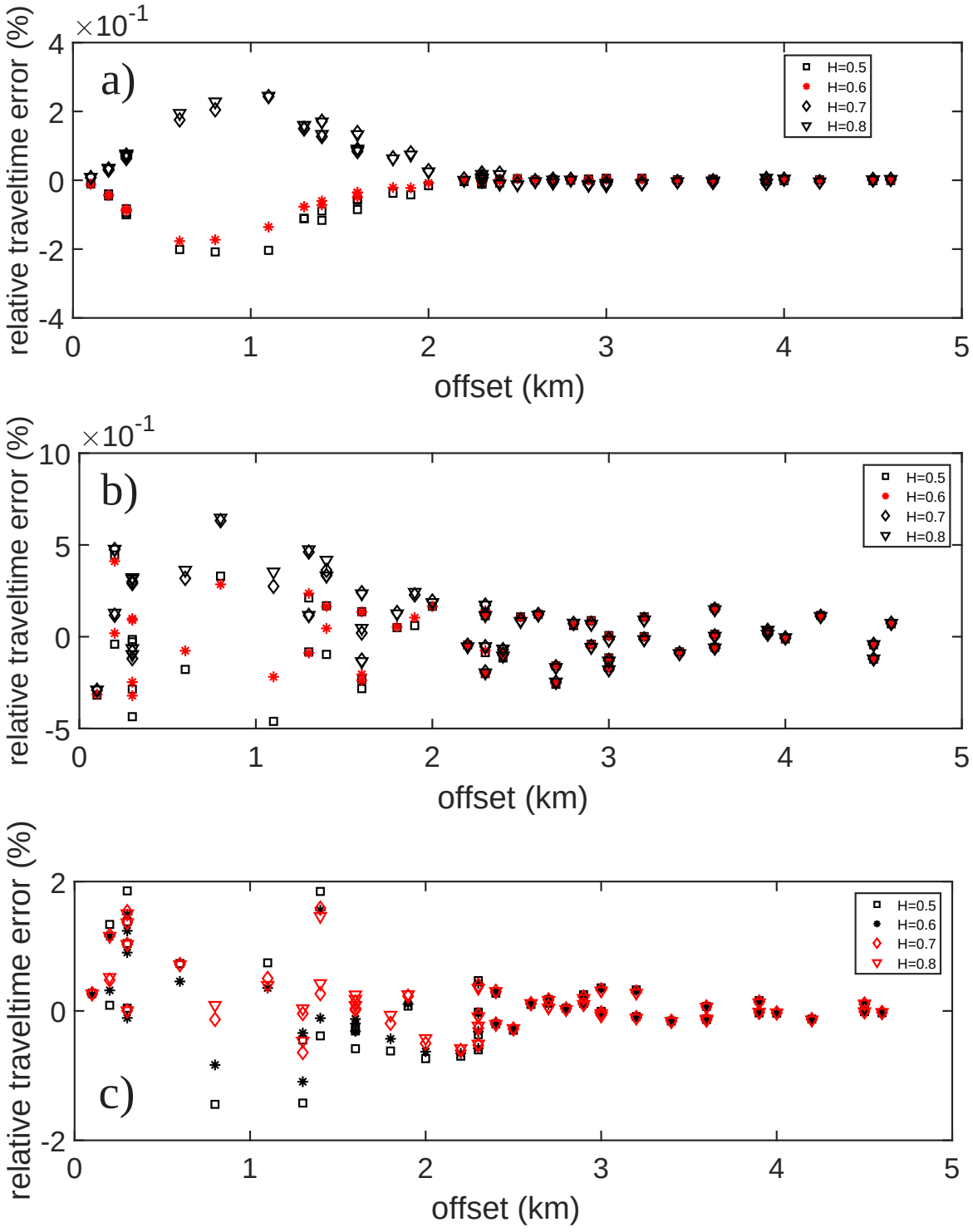

Figure 2: Relative traveltime erros $(T - T_{obs})/T_{obs}$ versus offset for the Model A for thickness H varying from 0.5 to 0.8 km. a) No noise, b) 2 ms and c) 4 ms random Gaussian noise added to traveltimes generated by ANRAY package. Red symbols indicate thicknesses with minimum sum of relative traveltime errors, see equation (9).

Variation of estimated A-parameters in the dependence on the assumed layer thickness H for the data with 2 ms random noise is shown in Table 1. The first line shows true values of the thickness H and of nine involved A-parameters. On the following lines, one can see the estimated values of A-parameters for thicknesses H varying from $H = 0.5$ to 0.8 km. The varying thickness has negligible effect on the estimates of ϵ_x, ϵ_y and η_z. Slightly stronger effect can be observed on A-parameters χ_z, ξ_{16} and ξ_{26}. Variation of H has significant effect on η_x and η_z, and also on ϵ_z. The effect of varying value of H on ϵ_z results from equation (6), in which ϵ_z depends on H through T_0. Comparison of estimated values of A-parameters for H=0.6 km with true parameters shows very good fit of all estimated A-parameters with true ones.

In Figure 3, comparison of true (red squares) and estimated (blue circles) A-parameters is shown. The blue vertical lines are the error bars introduced in Appendix B. The error bars are three times increased to make them clearly visible. Figure 3a shows results of the inversion of the noiseless traveltimes, Figures 3b and 3c show results with random Gaussian noise of 2 ms and 4 ms, respectively. Due to the weak anisotropy of the layer, we can see perfect fit of A-parameters estimated from noise-free data with true parameters in Figure 3a. Similar values of ϵ_x and ϵ_z and of η_x and η_z, and negligible value of η_z indicate that the studied medium is VTI. Introduction of noise affects mostly parameters η_x and η_y (see Table 1). It leads not only to a higher uncertainty of their determination, but also to their misfit with true values. Uncertainty also increases for parameters χ_z, ξ_{16} and ξ_{26}, but their misfit is small. The significant misfit of ϵ_z in Figure 3c is caused by incorrect estimate of H. Nevertheless, it is still obvious that we deal with a VTI layer. By comparing lines for $H = 0.6$ and 0.7 km in Table 1, one can see that the correct estimate of H would not improve estimates of A-parameters much, of course, except ϵ_z.

An interesting conclusion from the above test is that the detection of the model as VTI allows an approximate reconstruction of its phase velocity. For its reconstruction, it is sufficient to know three A-parameters, ϵ_x, δ_y and ϵ_z. The result of such reconstruction is shown in Figure 4b. In Figure 4a, the approximate phase-velocity surface calculated from true A-parameters (see the first line of Table 1) is shown as a reference. The phase-velocity surface shown in Figure 4b is reconstructed from A-parameters estimated from traveltimes with 2 ms random Gaussian noise (see the third line of Table 1). Very good fit of both surfaces is obvious.

As a next model, Model B, we took again the TI model whose matrix of density-normalized elastic moduli in the crystal coordinate system is shown in equation (C-1). In Model B, the axis of symmetry is inclined by 20° from vertical in the plane (z_1, z_3). We thus consider the TTI layer. Its thickness is 0.4 km. The true values of corresponding involved A-parameters can be found in Table 2. The rest of Table 2 shows, as in the case of Model A, values of A-parameters estimated from traveltimes with 2 ms random Gaussian noise for varying thickness H of the layer. Comparison of true parameters in Tables 1 and 2 shows that the only more distinct difference between models A and B are different values of A-parameters η_x and η_y.

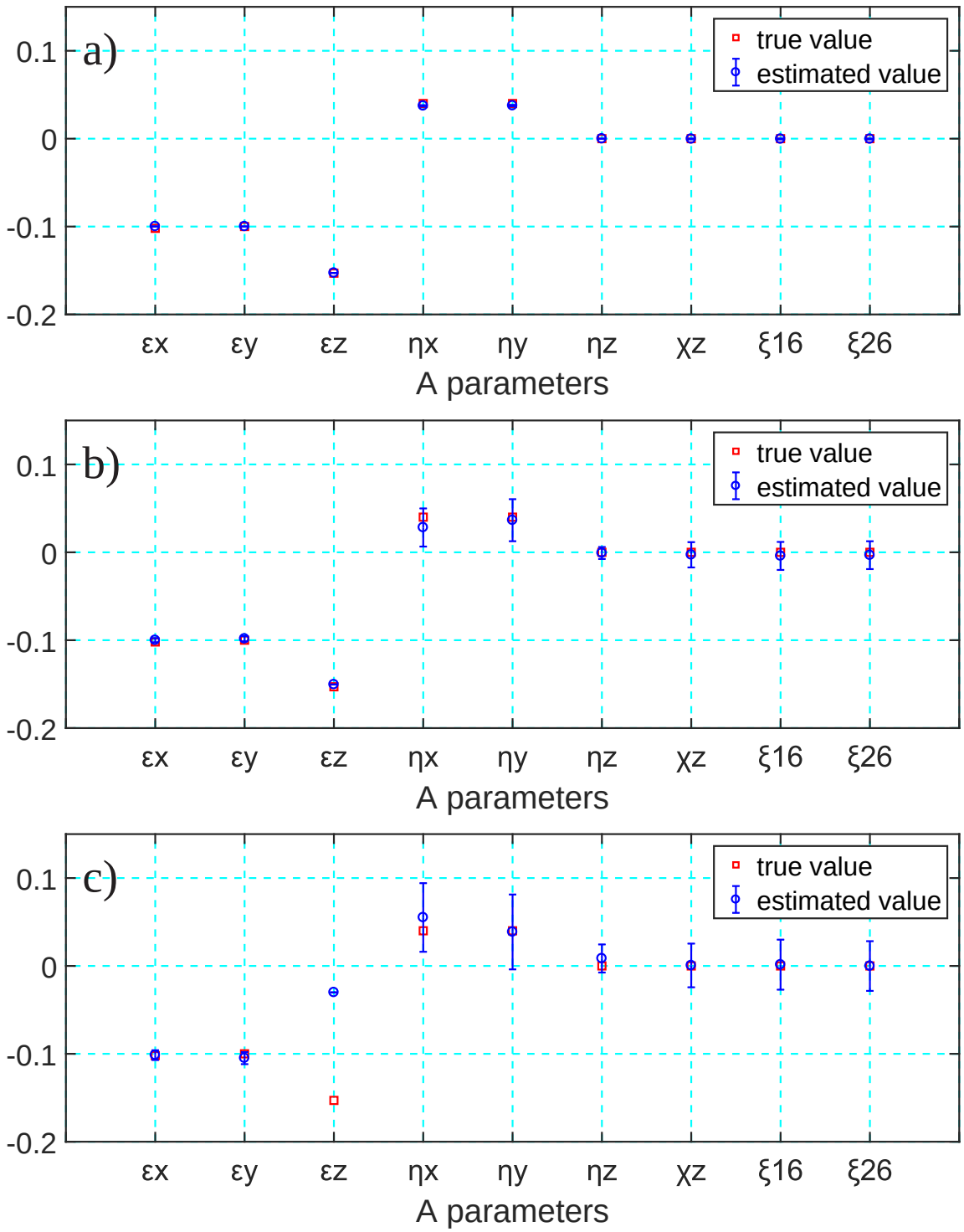

Figure 3: Results of the inversion of traveltime data generated in model A (VTI) with a) no noise, b) 2 ms and c) 4 ms random Gaussian noise added to traveltimes generated by ANRAY package. True (red squares) and estimated (blue circles) A-parameters. Blue vertical lines, error bars (3× exaggerated); reference velocity: $\alpha = 3.6$ kms. The thickness H of the layer estimated correctly in a) and b), $H = 0.6$ km; overestimated in c), $H = 0.7$ km.

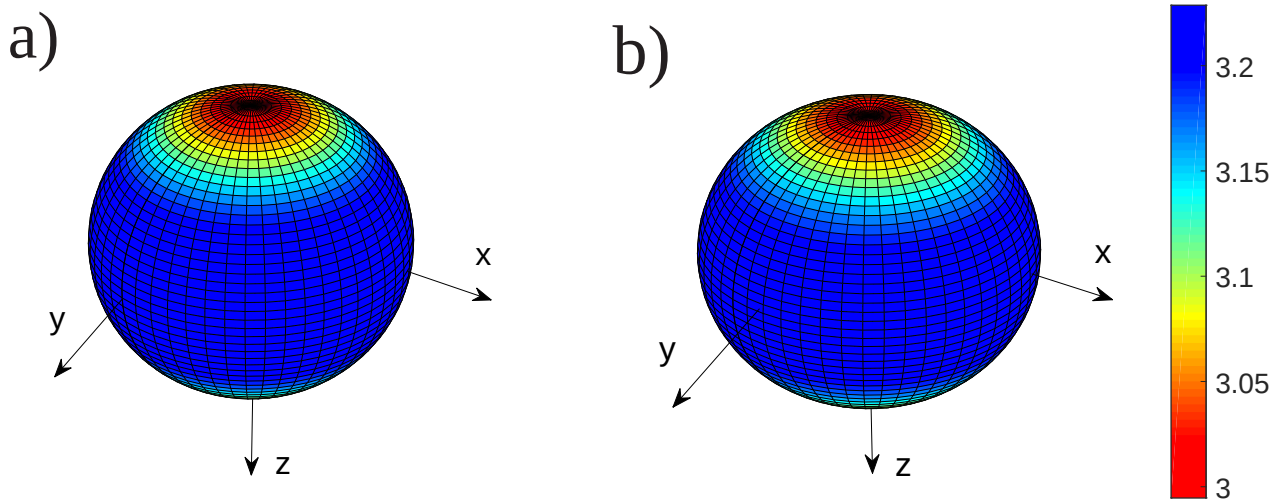

Figure 4: First-order P-wave phase velocity surfaces for model A calculated from a) true A-parameters; see the first line of Table 1 and b) parameters estimated from the inversion of traveltimes with 2 ms random Gaussian noise; see the third line of Table 1.

Model B	ϵ_x	ϵ_y	ϵ_z	η_x	η_y
	η_z	χ_z	ξ_{16}	ξ_{26}	
True	-0.102	-0.100	-0.143	0.031	0.007
$H = 0.4$ km	0.001	0.	0.	0.	
Estimated	-0.101	-0.101	-0.299	-0.108	-0.204
$H = 0.3$ km	-0.001	-0.011	-0.012	-0.013	
Estimated	-0.100	-0.101	-0.138	0.040	0.022
$H = 0.4$ km	-0.002	-0.007	-0.007	-0.008	
Estimated	-0.100	-0.101	0.066	-0.017	-0.066
$H = 0.5$ km	-0.002	-0.004	-0.004	-0.005	
Estimated	-0.098	-0.099	0.315	-0.216	-0.255
$H = 0.6$ km	-0.002	-0.007	-0.008	-0.009	

Table 2: True parameters and parameters estimated by inversion of traveltimes with 2 ms random Gaussian noise added to the data generated by ANRAY package in the model B. A-parameters ϵ_x, ϵ_y, ϵ_z, η_x, η_y, η_z, χ_z, ϵ_{16} and ϵ_{26} estimated for varying thickness of the layer H. P-wave reference velocity $\alpha = 3.6$ km/s.

The difference of η_x and η_y is also clearly observable in Figure 5a, showing the results of the inversion of noiseless traveltimes. As Figures 5b and 5c show, the estimates of η_x and η_y are strongly affected by noise. Nevertheless, the estimated values of η_x and η_y

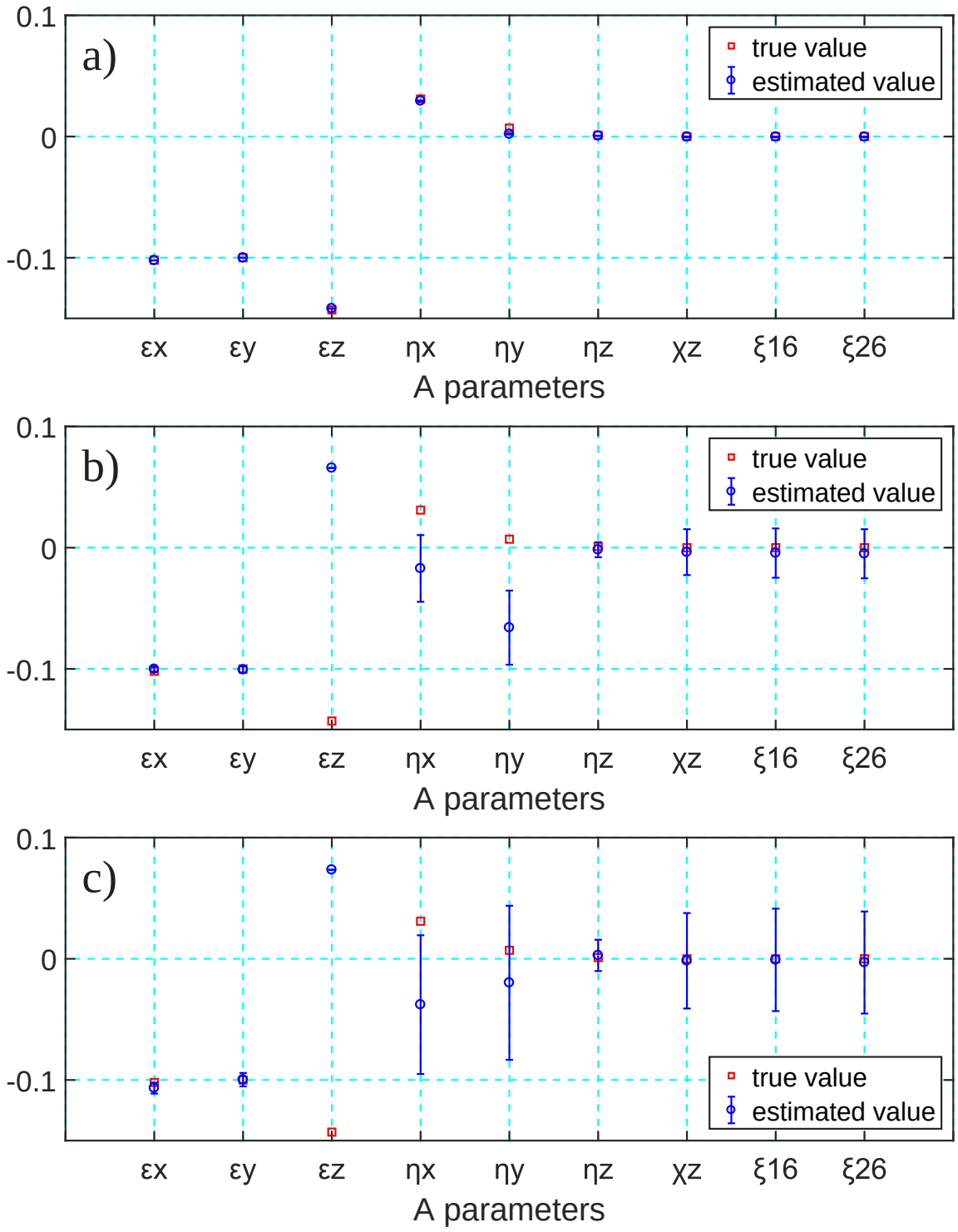

Figure 5: Results of the inversion of traveltime data generated in model B (TTI) with a) no noise, b) 2 ms and c) 4 ms random Gaussian noise added to traveltimes generated by ANRAY package. True (red squares) and estimated (blue circles) A-parameters. Blue vertical lines, error bars (3× exaggerated); reference velocity: $\alpha = 3.6$ kms. The thickness H of the layer estimated correctly in a) $H = 0.4$ km; overestimated in b) and c) $H = 0.5$ km.

differ, indicating that we do not deal with the VTI symmetry. The estimated values of η_x and η_y differ from their actual values. In comparison with Figure 3, A-parameters in Figure 5 are estimated with a greater uncertainty (greater error bars) for noisy traveltimes. In Figures 5b and 5c, we can also observe a great difference between estimated and true values of ϵ_z. The reason of the difference is the same as in Figure 3c, dependence of ϵ_z on the overestimated value of H, which affects ϵ_z through T_0 in equation (6).

So far we studied models of weak high-symmetry anisotropy. The models were transversely isotropic and their anisotropy did not exceed 10%. In the Model C, we consider an orthorhombic medium whose anisotropy is about 25%, which cannot be considered weak. As the model, we use the tilted orthorhombic medium proposed by Schoenberg and Helbig (1997). The thickness of the layer is $H = 0.5$ km. The 6×6 matrix of the density normalized elastic moduli in Voigt notation in the crystal coordinate system is shown in equation (C-2). In the Model C, the matrix is first rotated by 30° around the z_3-axis, and then by 20° around the new z_2 axis. Corresponding A-parameters in the global coordinate system are shown in Table 3 as true parameters. As in the previous cases, Table 3 shows values of A-parameters estimated from traveltimes with 2 ms random Gaussian noise for

Model C	ϵ_x	ϵ_y	ϵ_z	η_x	η_y
	η_z	χ_z	ξ_{16}	ξ_{26}	
True	-0.185	-0.154	-0.273	-0.063	-0.027
$H = 0.5$ km	0.048	0.004	0.010	0.052	
Estimated	-0.196	-0.134	-0.354	-0.334	-0.124
$H = 0.4$ km	-0.066	0.017	0.017	0.018	
Estimated	-0.195	-0.132	-0.274	-0.132	-0.013
$H = 0.5$ km	-0.072	0.009	0.009	0.010	
Estimated	-0.194	-0.129	-0.171	-0.064	-0.002
$H = 0.6$ km	-0.080	0.007	0.007	0.008	
Estimated	-0.192	-0.127	-0.052	-0.082	-0.059
$H = 0.7$ km	-0.090	0.005	0.006	0.006	

Table 3: True parameters and parameters estimated by inversion of traveltimes with 2 ms random Gaussian noise added to the data generated by ANRAY package in the model C. A-parameters ϵ_x, ϵ_y, ϵ_z, η_x, η_y, η_z, χ_z, ϵ_{16} and ϵ_{26} estimated for varying thickness of the layer H. P-wave reference velocity $\alpha = 3.6$ km/s.

varying thickness H of the layer. Comparison of the third line of Table 3 with its first line shows that the estimates of some of A-parameters in the Model C are of lower accuracy than in previous models. Greater differences are caused by significant strength of anisotropy of the Model C. It is also worth noting that the difference $|\epsilon - \delta|$ discussed by Xiao et al. (2004) exceeds the value of 0.2 in this case. Greater differences between estimated and true A-parameters can also be seen in Figure 6, which shows comparison of true A-parameters and their estimates with corresponding uncertainties from traveltimes

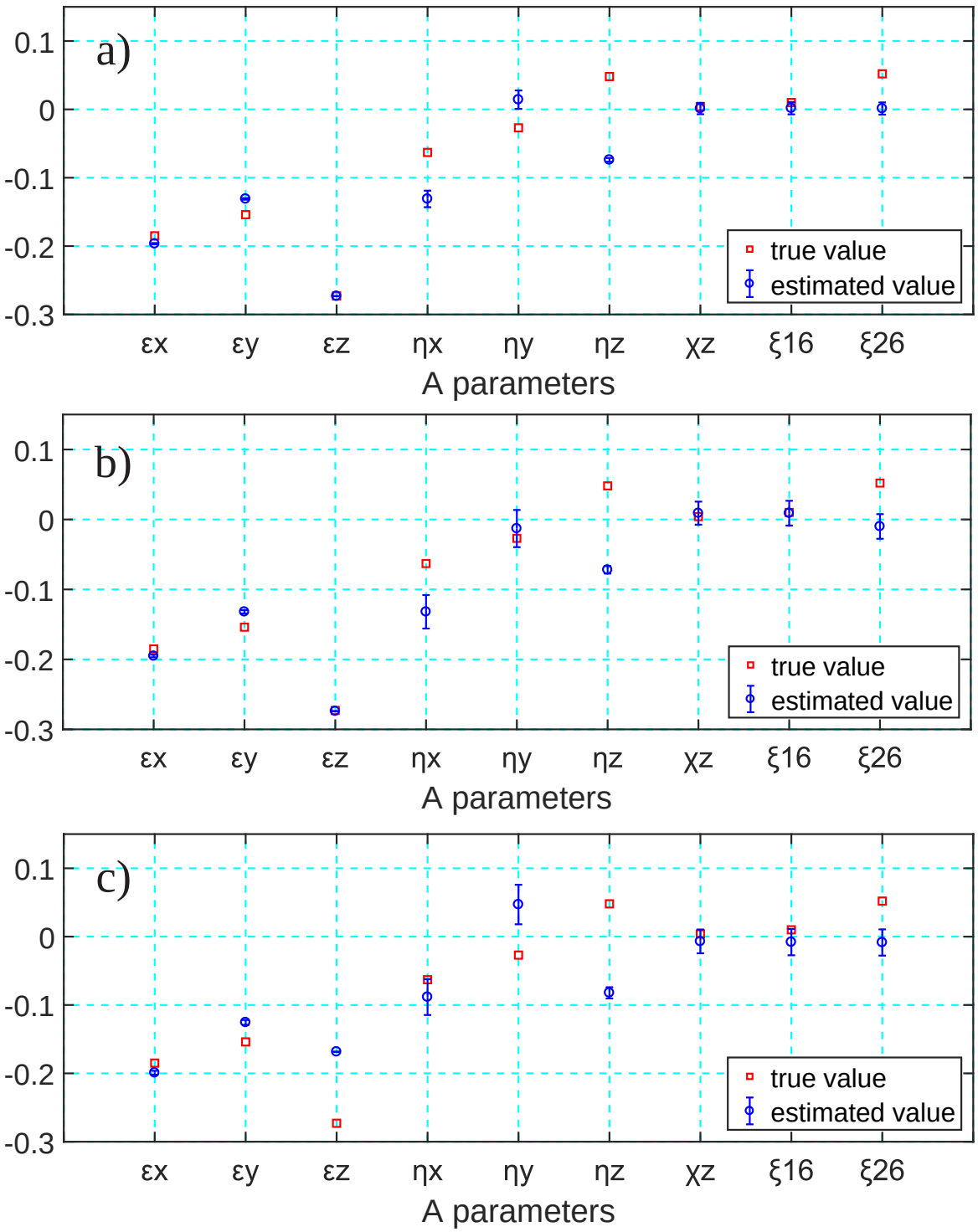

Figure 6: Results of the inversion of traveltime data generated in model C (ORT) with a) no noise, b) 2 ms and c) 4 ms random Gaussian noise added to traveltimes generated by ANRAY package. True (red squares) and estimated (blue circles) A-parameters. Blue vertical lines, error bars (3× exaggerated); reference velocity: $\alpha = 3.6$ kms. The thickness H of the layer estimated correctly in a) and b), $H = 0.5$ km; overestimated in c) $H = 0.6$ km.

with a) no, b) 2 ms and c) 4 ms random Gaussian noise. Greatest misfit can be observed in η parameters. Parameters ϵ_x, ϵ_y and ϵ_z, on the other hand, display relatively good fit. The misfit of the parameter ϵ_z in Figure 6c is again caused by the overestimate of H. Let us note again that similarly as in the TI case, it would be possible to reconstruct the phase-velocity if the orientation of the symmetry elements of the medium were known.

The last model, Model D, is a model of anisotropy of lowest symmetry, triclinic. The 6×6 matrix of the density normalized elastic moduli in Voigt notation specifying the model D is shown in equation (C-3). The model was proposed by Grechka (2020). The thickness of the layer is $H = 0.7$ km. The involved true A-parameters of this model are shown in the first line of Table 4. The rest of Table 4 shows values of A-parameters estimated from traveltimes with 2 ms random Gaussian noise for varying thickness H of the layer. Comparison of the first and third lines of Table 4, which correspond to the same thickness H, shows that the fit of estimated values of A-parameters with the values of true A-parameters is much better in the Model D than in the Model C. Except A-parameters ϵ_{16} and ϵ_{26}, the fit is very good. This clearly indicates that the main cause of significant misfit of estimated and true parameters in the Model C was the anisotropy strength of the Model C. Anisotropy symmetry does not play significant role.

Model D	ϵ_x	ϵ_y	ϵ_z	η_x	η_y
	η_z	χ_z	ξ_{16}	ξ_{26}	
True	0.264	0.495	0.298	0.015	0.389
$H = 0.7$ km	-0.091	0.015	-0.059	0.083	
Estimated	0.262	0.487	0.088	-0.149	0.322
$H = 0.6$ km	-0.104	-0.053	0.	-0.112	
Estimated	0.257	0.491	0.301	0.017	0.343
$H = 0.7$ km	-0.117	-0.041	0.018	-0.105	
Estimated	0.256	0.494	0.546	0.039	0.256
$H = 0.8$ km	-0.133	-0.031	0.036	-0.101	
Estimated	0.246	0.499	0.823	-0.068	0.061
$H = 0.9$ km	-0.155	-0.025	0.050	-0.103	

Table 4: True parameters and parameters estimated by inversion of traveltimes with 2 ms random Gaussian noise added to the data generated by ANRAY package in the model D. A-parameters ϵ_x, ϵ_y, ϵ_z, η_x, η_y, η_z, χ_z, ϵ_{16} and ϵ_{26} estimated for varying thickness of the layer H. P-wave reference velocity $\alpha = 3.6$ km/s.

Figure 7 confirms the above observations. The fit of ϵ_x, ϵ_y and even of η_x is perfect for all levels of noise. The misfit of the parameter ϵ_z in Figure 7c is caused again by the overestimate of the thickness H. In this case, the reconstruction of the phase-velocity surface would be impossible because inversion of equations (5) or (7) with (6) provides an incomplete set of P-wave A-parameters. For the reconstruction of the P-wave phase-velocity surface, fifteen P-wave A-parameters would be necessary, see Pšenčík et al., (2018, 2020).

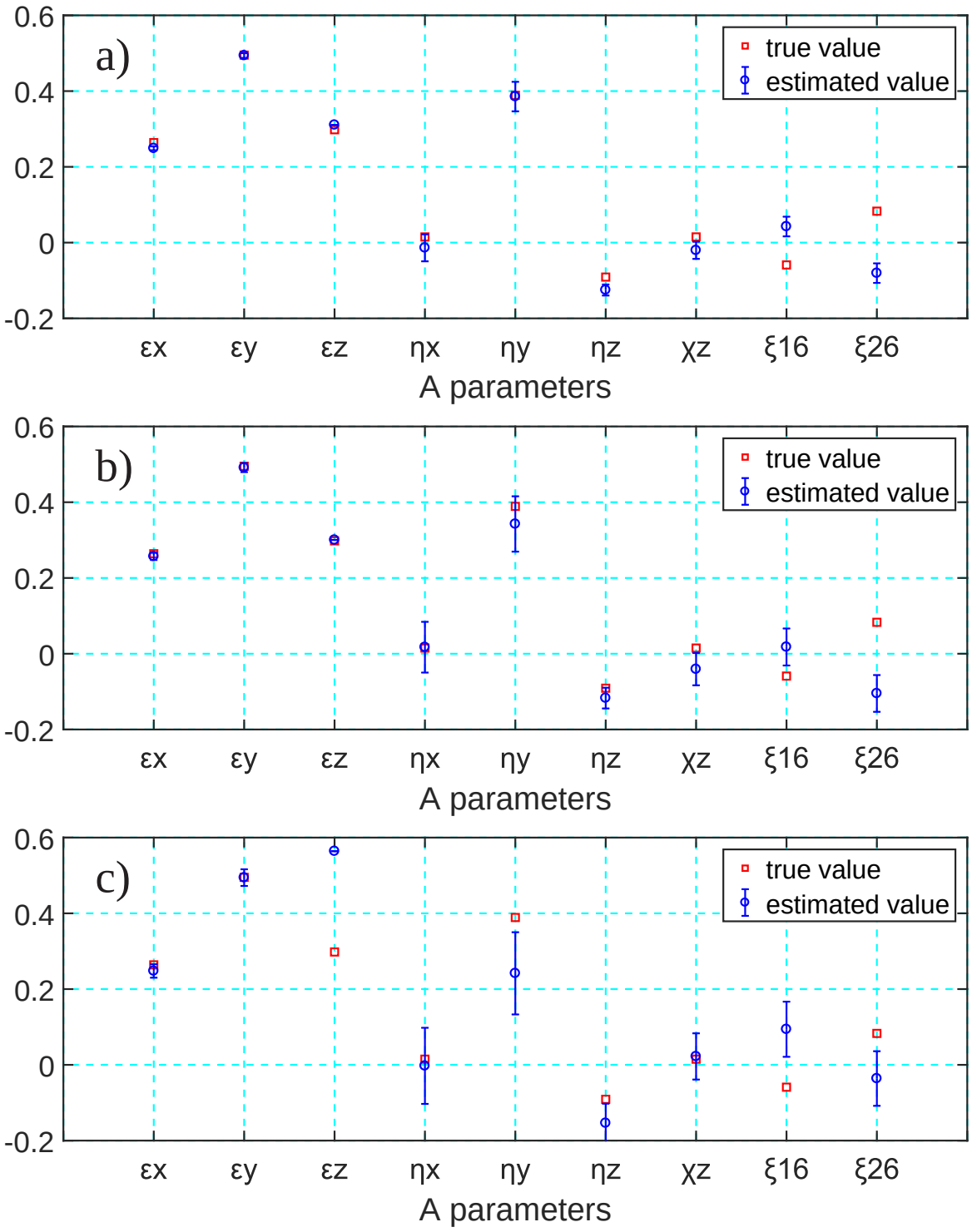

Figure 7: Results of the inversion of traveltime data generated in model C (ORT) with a) no noise, b) 2 ms and c) 4 ms random Gaussian noise added to traveltimes generated by ANRAY package. True (red squares) and estimated (blue circles) A-parameters. Blue vertical lines, error bars (3× exaggerated); reference velocity: $\alpha = 3.6$ kms. The thickness H of the layer estimated correctly in a) and b), $H = 0.7$ km; overestimated in c) $H = 0.8$ km.

Conclusion

Two inversion schemes for the approximate estimate of the thickness of a layer and some of its anisotropy parameters from the spatial distribution of traveltimes of P wave reflected from the bottom of the layer are proposed. In one of the schemes, nine A-parameters ϵ_x, ϵ_y, ϵ_z, η_x, η_y, η_z, ξ_{16}, ξ_{26} and χ_z are sought, possibly together with the thickness of the layer H. In the other scheme, the A-parameter ϵ_z is estimated separately from the observed zero-offset traveltime. The latter scheme is tested by inverting traveltimes of P waves reflected at the bottom of homogeneous layers of varying anisotropy symmetry and strength. The tests indicate that the inversion scheme is applicable to any anisotropy symmetry. The accuracy of the values of estimated A-parameters decreases with the anisotropy strength. Nevertheless, the test with the model with anisotropy strength exceeding 20% can still yield reasonable estimates of A-parameters.

Successful recovery of the involved A-parameters depends also on the offset of the used receivers. Numerical tests indicate that sufficiently accurate estimates of the thickness H of a layer and of its A-parameters can be obtained if normalized offsets $\bar{x}$ attain values of, at least, 3.5 to 4.

A-parameters ϵ_x and ϵ_y are usually estimated best and with least uncertainty. The same hold for ϵ_z if a correct estimate of the thickness H is used. Parameters ϵ_x and ϵ_y are also least sensitive to the variation of the thickness H. On the contrary most unreliable parameters with greatest uncertainties are parameters η.

As mentioned above, the proposed procedure does allow estimation of not only A-parameters, but also of the thickness H of the layers. Approximate character of the inversion formula is responsible for the tendency of the procedure to overestimate the true thickness. The chance for an overestimate increases with increasing level of noise in traveltimes. The whole procedure can be simplified considerably if the thickness of the layer is a priori known. This simplifies the inversion procedure considerably because it avoids the iterative part, within which A-parameters are sought for varying values of H.

In case of higher-symmetry anisotropy, additional information about symmetry can help to estimate additional A-parameters and to reconstruct the phase velocity surface of the studied medium. As shown in the text, such a surface can be reconstructed even without knowledge of additional parameters if we deal, for example, with a VTI symmetry.

The proposed inversion procedure clearly demonstrates the advantage of the parameterization of a medium by A-parameters. The same set of A-parameters can be used for the description of any anisotropy symmetry.

The procedure could be extended to the inversion of traveltimes of converted PSV waves reflected from the bottom of a VTI layer. Extension to lower-symmetry anisotropic media would probably require the use of the common S-wave concept, which may turn problematic.

Acknowledgement

We are grateful to Luděk Klimeš and Sláva Růžek for useful comments. Han Xiao is sponsored by Chinese Scholarship Council No. 201906170237. We thank the project "Seismic waves in complex 3-D structures" (SW3D) and Research Project 20-06887S of the Grant Agency of the Czech Republic for support.

Appendix A

P-wave profile A-parameters
and their expression in terms of global A-parameters

A-parameters are a generalization of Thomsen (1986) VTI parameters for arbitrary anisotropy. The commplete set of 21 A-parameters (Pšenčík et al., 2018) represents an alternative to 21 independent elements of the stiffness tensor. They can be used for the description of anisotropy of arbitrary symmetry and strength. In the weak-anisotropy approximation, used in this paper, P-wave propagation is described by only fifteen P-wave A-parameters. For the solution of the problem of this paper, only nine A-parameters, used in equatons (5) and (7) and defined below, are sufficient.

Along each profile, moveout formula (1) depends on three P-wave profile A-parameters ϵ_x^P, η_y^P and ϵ_z^P defined as follows:

$$\epsilon_x^P = \frac{A_{11}^P - \alpha^2}{2\alpha^2} \ , \quad \epsilon_z^P = \frac{A_{33}^P - \alpha^2}{2\alpha^2} \ , \quad \eta_y^P = \frac{2(A_{13}^P + 2A_{55}^P) - A_{11}^P - A_{33}^P}{2\alpha^2} \ . \qquad (A-1)$$

We use upper indices P in order to distinguish the profile parameters from the global A-parameters defined in the global coordinate system and presented below. The profile A-parameters (A-1) are expressed in terms of four density-normalized elastic parameters $A_{\alpha\beta}^P$ related to the given profile, and a constant reference P-wave velocity α.

Let us now assume that the profile makes an angle φ with the z_1 axis of the global coordinate system. P-wave profile A parameters ϵ_x^P, η_y^P and ϵ_z^P defined in equation (A-1) could be then expressed generally in terms of fifteen P-wave global A-parameters. It is possible to show, see, for example, Pšenčík and Farra (2017), that the depndence on six of the fifteen P-wave global A-parameters is negligible. It is thus sufficient to consider the dependence on only nine of fifteen global P-wave A-parameters:

$$\epsilon_x = \frac{A_{11} - \alpha^2}{2\alpha^2} \ , \quad \epsilon_y = \frac{A_{22} - \alpha^2}{2\alpha^2} \ , \quad \epsilon_z = \frac{A_{33} - \alpha^2}{2\alpha^2} \ , \quad \eta_x = \frac{2(A_{23} + 2A_{44}) - A_{22} - A_{33}}{2\alpha^2} \ ,$$

$$\eta_y = \frac{2(A_{13} + 2A_{55}) - A_{33} - A_{11}}{2\alpha^2} \ , \quad \eta_z = \frac{2(A_{12} + 2A_{66}) - A_{11} - A_{22}}{2\alpha^2} \ ,$$

$$\chi_z = \frac{A_{36} + 2A_{45}}{\alpha^2} \ , \quad \xi_{16} = \frac{A_{36} + 2A_{45} - A_{16}}{\alpha^2} \ , \quad \xi_{26} = \frac{A_{36} + 2A_{45} - A_{26}}{\alpha^2} \ . \qquad (A-2)$$

The profile A-parameters (A-1) can be expressed in terms of the above nine global A-parameters using the following transformation formulae:

$$\epsilon_x^P = \epsilon_x \cos^2\varphi + \epsilon_y \sin^2\varphi + \eta_z \cos^2\varphi \sin^2\varphi + 2\chi_z \cos\varphi \sin\varphi$$

$$-2\xi_{16} \cos^3\varphi \sin\varphi - 2\xi_{26} \cos\varphi \sin^3\varphi \ ,$$

$$\epsilon_z^P = \epsilon_z \ ,$$

$$\eta_y^P = \eta_x \sin^2\varphi + \eta_y \cos^2\varphi - \eta_z \cos^2\varphi \sin^2\varphi + 2\xi_{16} \cos^3\varphi \sin\varphi + 2\xi_{26} \cos\varphi \sin^3\varphi \ . \quad (A-3)$$

The above transformation equations represent the Bond transformation (Bond, 1943; Chapman, 2004) expressed in terms of A-parameters.

Appendix B

Inversion scheme

We start with equation (8):

$$\mathbf{Gm} = \mathbf{d}. \qquad (B-1)$$

The symbol $\mathbf{G}$ represents the $N \times M$ matrix, where N is the number of observations and M is the number of sought A-parameters. In our case $M = 8$. The rows of matrix $\mathbf{G}$ have the following form:

$$\bar{x}^2(1+\bar{x}^2)\cos^2\varphi \quad \bar{x}^2(1+\bar{x}^2)\sin^2\varphi \quad \bar{x}^2\sin^2\varphi \quad \bar{x}^2\cos^2\varphi \quad \bar{x}^4\cos^2\varphi\sin^2\varphi$$

$$2\bar{x}^2(1+\bar{x}^2)\cos\varphi\sin\varphi \quad 2\bar{x}^4\cos^3\varphi\sin\varphi \quad 2\bar{x}^4\cos\varphi\sin^3\varphi\ . \qquad (B-2)$$

Each row in matrix $\mathbf{G}$ corresponds to one particular ray of the reflected wave.

Symbol $\mathbf{m}$ in equation (B-1) is the eight-dimensional vector of model parameters to be determined. It consists of eight P-wave A parameters m_i ordered as:

$$\mathbf{m} \equiv (\epsilon_x \quad \epsilon_y \quad \eta_x \quad \eta_y \quad \eta_z \quad \xi_x \quad \xi_{16} \quad \xi_{26})^T\ . \qquad (B-3)$$

The symbol T indicates transposition.

Vector $\mathbf{d}$ in equation (B-1) has the following form:

$$\mathbf{d} \equiv \frac{1}{2}\Big((1+\bar{x}_1^2)\Big[\Big(\frac{T_0^2(1+\bar{x}_1^2)}{T_{obs}^2(x_1)} - 1\Big)(1+\bar{x}_1^2) - \frac{T_0^2 - T_{obs}^2(0)}{T_{obs}^2(0)}\Big]$$

$$(1+\bar{x}_2^2)\Big[\Big(\frac{T_0^2(1+\bar{x}_2^2)}{T_{obs}^2(x_2)} - 1\Big)(1+\bar{x}_2^2) - \frac{T_0^2 - T_{obs}^2(0)}{T_{obs}^2(0)}\Big] \qquad ....$$

$$(1+\bar{x}_N^2)\Big[\Big(\frac{T_0^2(1+\bar{x}_N^2)}{T_{obs}^2(x_N)} - 1\Big)(1+\bar{x}_N^2) - \frac{T_0^2 - T_{obs}^2(0)}{T_{obs}^2(0)}\Big]\Big)^T\ . \qquad (B-4)$$

Equation (B-1) can be solved by pseudoinverse (e.g., Press et al., 2007; Aster et al., 2013):

$$\mathbf{m} = \mathbf{G}^\dagger\mathbf{d}, \qquad (B-5)$$

where $\mathbf{G}^\dagger$ denotes the pseudoinverse of matrix $\mathbf{G}$.

An important part of the inversion is the assessment of errors of estimated A-parameters. We follow here Pšenčík et al. (2020) and transform the data covariance matrix $\mathbf{C}_d$ to the model covariance matrix $\mathbf{C}_m$:

$$\mathbf{C}_m = \mathbf{G}^\dagger\mathbf{C}_d\mathbf{G}^{\dagger T}\ . \qquad (B-6)$$

Instead of the unknown exact data covariance matrix $\mathbf{C}_d$, we use its approximation:

$$\mathbf{C}_d \approx \sigma^2\mathbf{I}, \qquad (B-7)$$

where $\mathbf{I}$ is the 8×8 identity matrix. The value of the parameter σ is determined using χ^2 statistics of residuals $\mathbf{r} = \mathbf{d} - \mathbf{Gm}$ with the number of degree of freedom $\nu = N - M$. We get

$$\sigma = \sqrt{\nu^{-1}\mathbf{r}^T\mathbf{r}}\ , \qquad (B-8)$$

see equation (A-10) of Pšenčík et al. (2020).

Using equation (B-6), we can estimate the model covariance matrix $\mathbf{C}_m$. Square roots of diagonal elements of $\mathbf{C}_m$ then represent Gaussian errors of individual A-parameters expressed as error bars in the estimates of A-parameters. Note that the Gaussian error of the A-parameter ϵ_z is zero because ϵ_z is calculated exactly from equation (6).

Appendix C

Matrices of the used density-normalized elastic moduli

The matrix of the density-normalized elastic moduli in $(\mathrm{km/s})^2$ of limestone with the vertical axis of symmetry, used in Model A (Farra and Pšenčík, 2020):

$$\begin{pmatrix} 10.368 & 4.540 & 4.369 & 0 & 0 & 0 \\ & 10.368 & 4.369 & 0 & 0 & 0 \\ & & 9.000 & 0 & 0 & 0 \\ & & & 2.914 & 0 & 0 \\ & & & & 2.914 & 0 \\ & & & & & 2.914 \end{pmatrix}. \qquad (C-1)$$

Anisotropy strength of the model is about 8%.

The matrix of the density-normalized elastic moduli in $(\mathrm{km/s})^2$ of the model of orthorhombic symmetry, used in Model C (Schoenberg and Helbig, 1997):

$$\begin{pmatrix} 9.000 & 3.600 & 2.250 & 0 & 0 & 0 \\ & 9.840 & 2.400 & 0 & 0 & 0 \\ & & 5.938 & 0 & 0 & 0 \\ & & & 2.000 & 0 & 0 \\ & & & & 1.600 & 0 \\ & & & & & 2.182 \end{pmatrix}. \qquad (C-2)$$

Anisotropy strength of the model is about 25%.

The matrix of the density-normalized elastic moduli in $(\mathrm{km/s})^2$ of the model of triclinic symmetry, used in Model D (Grechka, 2020):

$$\begin{pmatrix} 19.810 & 8.620 & 9.000 & -2.370 & -1.440 & 0.950 \\ & 25.790 & 9.090 & 0.570 & -0.990 & -0.890 \\ & & 20.680 & -2.100 & 0.430 & 0.490 \\ & & & 7.170 & -0.150 & -0.080 \\ & & & & 8.140 & -0.330 \\ & & & & & 6.490 \end{pmatrix}. \qquad (C-3)$$

References

Aster, R. C., B. Borchers, and C. H. Thurber, 2013. Parameter estimation and inverse problems: Academic Press, Oxford.

Bond, W., 1943, The mathematics of the physical properties of crystals: Bell System Technical Journal, **22**, 1–72, doi: 10.1002/j.1538-7305.1943.tb01304.x.

Chapman, C. H., 2004, Fundamentals of seismic wave propagation: Cambridge University Press.

Farra, V., and I. Pšenčík, 2016, Weak-anisotropy approximations of P-wave phase and ray velocities for anisotropy of arbitrary symmetry: Studia Geophysica et Geodaetica, **60**, 403-418.

Farra, V., and I. Pšenčík, 2020, P-wave reflection-moveout approximation for horizontally layered media of arbitrary moderate anisotropy: Geophysics, **85**, C61–C70.

Gajewski, D., and I. Pšenčík, 1990, Vertical seismic profile synthetics by dynamic ray tracing in laterally varying layered anisotropic structures: J. Geophys. Res., **95**, 11301–11315.

Grechka, V., 2020, Moment tensors of double-couple microseismic sources in anisotropic formations: Geophysics, **85**, 1JF–Z3.

Press, W. H., B. P. Flannery, S. A. Teukolsky, and W. T. Vetterling, 2007. Numerical recipes: Cambridge University Press, Cambridge.

Pšenčík, I., 2017, Transformation rules for weak-anisotropy parameters: Seismic waves in Complex 3-D Structures, 27, 59–68, online at "http://sw3d.cz".

Pšenčík, I., and V. Farra, 2017, Reflection moveout approximations for P-waves in a moderately anisotropic homogeneous tilted transverse isotropy layer: Geophysics, **82**, C175-C185.

Pšenčík, I., B. Růžek, T. Lokajíček, and T. Svitek, 2018, Determination of rock-sample anisotropy from P- and S-wave traveltime inversion: Geophys. J. Int., **214**, 1088–1104.

Pšenčík, I., B. Růžek, P. Jílek, 2020, Practical concept of traveltime inversion of simulated P-wave vertical seismic profile data in weak to moderate arbitrary anisotropy: Geophysics, **85**, C107–C123.

Schoenberg, M., and K. Helbig, 1997, Orthorhombic media: Modeling elastic wave behavior in a vertically fractured earth. Geophysics, **62**, 1954–1974.

Thomsen, L., 1986, Weak elastic anisotropy: Geophysics, **51**, 1954–1966.

Xiao, Ch, J.C.Bancroft, and R.J. Brown 2004, Estimation of anisotropy parameters in VTI media: SEG Expanded Abstracts, https://doi.org/10.1190/1.1851093.